Ternary Cluster Anions

DOI: 10.1002/anie.201005496

Neither Electron-Precise nor in Accordance with Wade–Mingos Rules: The Ternary Cluster Anion $[Ni_2Sn_7Bi_5]^{3-}$**

*Felicitas Lips and Stefanie Dehnen**

Dedicated to Professor Hansgeorg Schnöckel on the occasion of his 70th birthday

During the past decade it has been shown that embedding d^{10} transition metal atoms may help to stabilize anionic main-group-element cages that would not otherwise be stable. These so-called intermetalloid cluster anions possess a number of chemical and physical peculiarities that made them highly attractive and challenging to both synthetic chemists and theorists.[1,2] For example, owing to the interstitial atom, the surrounding cages tend to exceed the size limit of nine atoms for isolated Zintl anions, as observed in $[M@Pb_{10}]^{2-}$,[3] $[M@Pb_{12}]^{2-}$,[3] (M = Ni, Pd, Pt), or $[Pd_2@Ge_{18}]^{4-}$.[4] The resulting clusters can also exhibit onion-type structures, as observed in icosahedral $[As@Ni_{12}@As_{20}]^{3-}$.[5] The electronic situation of the intermetalloid cages is not trivial. In some cases, the anions are in accordance with Wade–Mingos rules,[6] such as $[M@Pb_{10}]^{2-}$ or $[M@Pb_{12}]^{2-}$, but frequently, the simple and otherwise very strong concept for the correlation of structures and electron numbers fails. An uncommon count of ligand donor electrons, as discussed for $[Zn_9Bi_{11}]^{5-}$,[7] may be needed to match the electron numbers. Recently, transition metals with open d shells have also been useful to construct intermetalloid cluster anions with non-deltahedral architectures, namely $[Fe@Ge_{10}]$[8] and $[Co@Ge_{10}]$,[9] which are thus no longer Wade–Mingos clusters.

Another extension of the field has been achieved recently in our group by generating ternary Zintl anions $[Zn_6Sn_3Bi_8]^{4-}$[10] and $[Sn_2Sb_5(ZnPh)_2]^{3-}$,[11] the latter of which belongs to a type of intermetalloid clusters with the transition metal complex fragment contributing to the cluster surface. The compounds demonstrated the influence of the new degree of freedom in the electron number on the cage structures. Group 14 (E^{14}) or Group 15 (E^{15}) elements usually form different homoatomic or binary intermetalloid Zintl anions. Therefore, mixtures of binary E^{14}/E^{15} Zintl anions or ternary intermetalloid $M/E^{14}/E^{15}$ Zintl clusters may show analogies to one of the two separate systems or create new structural features to coincide with the new electronic situation. The above-mentioned ternary products with M = Zn were different from binary intermetalloid clusters, but were more similar to previously reported homoatomic or intermetalloid Zintl anions with Group 15 elements. As with $[Zn_9Bi_{11}]^{5-}$, $[Zn_6Sn_3Bi_8]^{4-}$ could be comprehended in terms of Wade–Mingos rules, if treated in a suitable way.

Herein we report the synthesis of a novel compound that comprises a ternary Zintl anion that a) fails both a localized bonding description and Wade–Mingos rules by two electrons and b) shows more similarities to previous results with Group 14 elements: $[K([2.2.2]crypt)]_3[Ni_2Sn_7Bi_5]\cdot 1.8\,en\cdot 2\,tol$ (**1**; en = 1,2-ethylenediamine, tol = toluene) was obtained by reaction of $[K([2.2.2]crypt)]_2[Sn_2Bi_2]\cdot en$[12] with $[Ni(cod)_2]$ (cod = 1,5-cyclooctadiene) as dark brown crystals (yield 15%) along with the crystalline starting material (60%).

Figure 1 shows the molecular structure of the ternary intermetalloid cluster anion. In **1**, two interstitial Ni atoms form a dumbbell with a Ni–Ni bond of 244.4(2) pm that is embedded within a 12-atom Sn_7Bi_5 cage. The latter can be described as two tetragonal antiprisms that share a Sn_4 face (Sn5–8).

At first glance, the Sn/Bi cage resembles an *arachno* cluster, because a formally underlying 14-atom deltahedron is lacking two capping atoms. Thus, the anion in **1** has two

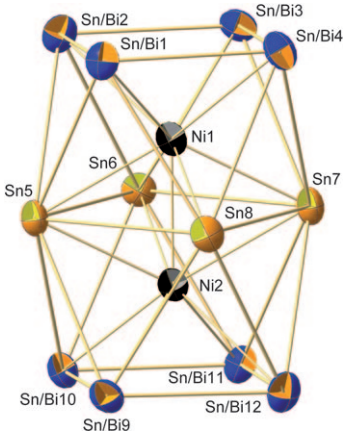

Figure 1. Structure of the anion in **1** (ellipsoids set at 50% probability); mixed blue/orange spheres indicate statistic atomic disorder of Sn and Bi. Selected interatomic distances [pm]: (Sn/Bi1–4)–(Sn/Bi1–4) 299.1(1)–301.8(1), (Sn/Bi9–12)–(Sn/Bi9–12) 299.6(1)–303.2(1), (Sn5–8)–(Sn5–8) 325.8(1)–332.3(1), (Sn/Bi1–4)–(Sn5–8) 328.6(1)–334.3(2), (Sn/Bi9–12)–(Sn5–8) 326.2(2)–333.6(2), Ni1–(Sn/Bi1–4) 265.1(2)–267.9(2), Ni2–(Sn/Bi9–12) 265.4(2)–267.7(2), Ni1–(Sn5–8) 262.7(2)–263.9(2), Ni2–(Sn5–8) 261.9(2)–263.9(2), Ni1–Ni2 244.4(2).

[*] F. Lips, Prof. Dr. S. Dehnen
Fachbereich Chemie und Wissenschaftliches Zentrum für Materialwissenschaften (WZMW), Philipps Universität Marburg
Hans-Meerwein-Strasse, 35043 Marburg (Germany)
Fax: (+49) 6421-282-5653
E-mail: dehnen@chemie.uni-marburg.de

[**] This work was supported by the Fonds der Chemischen Industrie (Chemiefonds-Stipendium for F.L.) and the DFG. We thank Dr. U. Linne and J. Bamberger for recording the ESI mass spectra.

Supporting information for this article is available on the WWW under http://dx.doi.org/10.1002/anie.201005496.

external non-deltahedral, square-planar faces (Sn/Bi1–4 and Sn/Bi9–12). To analyze the corresponding electron number, it is necessary to determine the Sn:Bi ratio, which is not trivial in this case, as the atomic sites of these faces are statistically occupied by Sn (site occupancy factor (sof) 0.46–0.41) and Bi atoms (sof 0.54–0.59). Statistic disorder of Sn and Bi was also observed for $[Zn_6Sn_3Bi_8]^{4-}$,[10] $[Sn_7Bi_2]^{2-}$,[10] and for the binary $[Sn_2Bi_2]^{2-}$ anion in the starting material.[12] Apart from a sophisticated single-crystal X-ray refinement procedure, the Sn:Bi ratio has been further supported by energy-dispersive X-ray (EDX) analysis (see the Supporting Information).

To gain more insight in the formation of the cluster and to understand the observation of a rather random distribution of Sn and Bi atoms, both the precursor solution in ethylenediamine and the reaction mixture were analyzed by ESI mass spectrometry (see the Supporting Information and Figure 2).[13] The starting material produces only one predominant peak at m/z 656.77, which corresponds to the protonated precursor anion $[Sn_2Bi_2H]^-$. However, upon adding the nickel complex, the situation changes dramatically. Although the precursor is still observable in small amounts in the reaction mixture, the strongest assignable signal derives from $[Bi_3Sn]^-$ (m/z 746.84), followed by $[Sn_6Bi_3]^-$ (m/z 1338.35), indicating fragmentation and rearrangement of the precursor anion.[14] A peak of relatively low intensity at m/z 1396.29 accords to the cluster fragment $[Sn_6Bi_3Ni]^-$. Regarding both literature data and our own experience,[10] it seems likely that the latter are unprecedented variants of topologically known nine-atom cages without[15] or with an interstitial nickel atom;[16] these might be viewed as intermediates at the formation of the larger cluster in **1**.

The complete anion of **1** does not seem to be present in the reaction mixture or in solutions of the single crystals in ethylenediamine, dimethylformamide, pyridine, or acetonitrile. Compound **1** appears to form reversibly during the crystallization process by further aggregation/rearrangement of cluster and precursor fragments.

We have performed quantum-chemical investigations using DFT methods[17] within the program system TURBOMOLE[18] for rationalization of both the Sn:Bi ratio and the unequal distributions of Sn and Bi atoms over the cluster atomic positions. For every possible composition, from $[Ni_2Sn_{12}]^{3-}$ to $[Ni_2Bi_{12}]^{3-}$, all possible isomers were calculated without symmetry restriction (see the Supporting Information). Those isomers which were the energetic minimum structures for the respective composition have been further used 1) for analysis of the structural parameters and 2) for calculation of reaction energies of a hypothetical reorganization reaction of two molecules of a given cluster composition into the two clusters with one Sn or Bi atom more or less [Eq. (1); $x = 1$–11; $x + y = 12$].

$$2\,[Ni_2Sn_xBi_y]^{3-} \rightarrow [Ni_2Sn_{x+1}Bi_{y-1}]^{3-} + [Ni_2Sn_{x-1}Bi_{y+1}]^{3-} \quad (1)$$

First, the proposed composition shows the best fit with experimental bond lengths (absolute deviation from −0.6 to +9.9 pm; average deviation from 0.95 to 6.45 pm). Second, analysis of the reaction energies as a function of the number of Sn atoms in the reactant species, x, illustrates that the according reaction of $[Ni_2Sn_7Bi_5]^{3-}$ is the most endoenergetic process by at least 20 kJ mol^{-1}, or by at least 88 kJ mol^{-1} if only reasonable structures are considered (Figure 3). Accordingly, this composition turns out to be favored over the other ones, which is in agreement with the experimental findings for

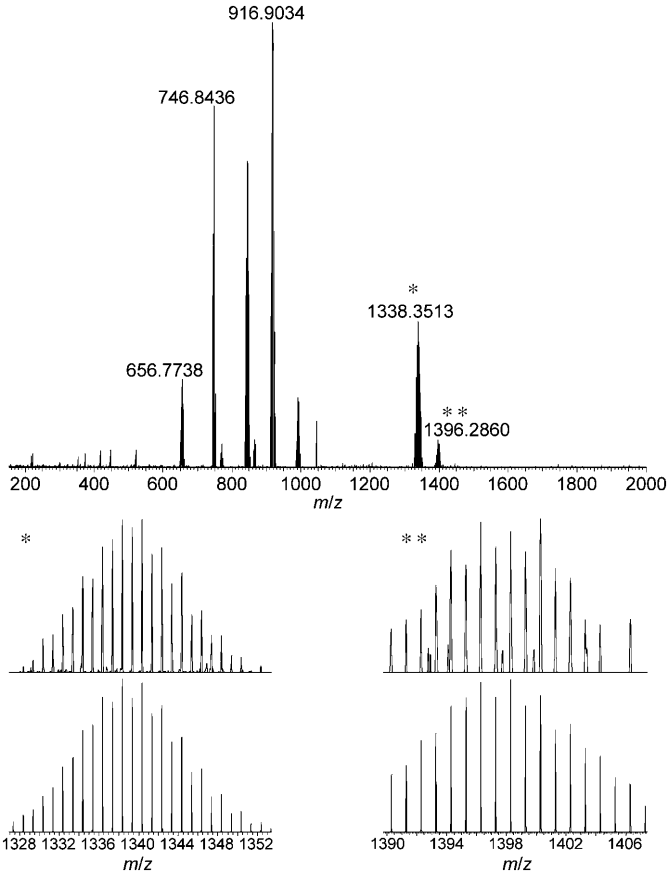

Figure 2. Top: Electrospray ionization mass spectrum of the reaction solution after 3 h reaction time. Bottom: Expansion of the observed and calculated signals of $[Sn_6Bi_3]^-$ (m/z 1338.35, marked by *) and $[Sn_6Bi_3Ni]^-$ (m/z 1396.29, marked by **).

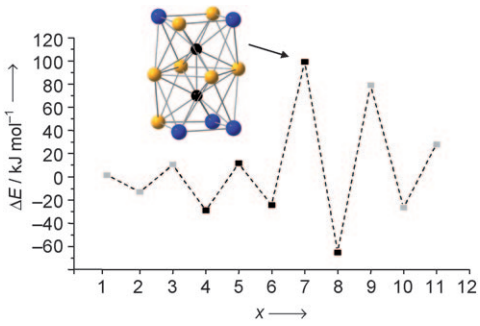

Figure 3. Energies for the hypothetical reactions given in equation (1) as a function of the number of tin atoms in the reactant x, and structure of the preferred isomer of $[Ni_2Sn_7Bi_5]^{3-}$ (Ni black, Sn orange, Bi blue). Gray squares indicate compositions that converge into geometries that disagree with the experimentally observed geometry, and are thus directly excluded. Calculations of $[Ni_2Sn_{12}]^{3-}$ and $[Ni_2Bi_{12}]^{3-}$ in D_{4h} symmetry resulted in the desired geometry, but represent saddle points as confirmed by analysis of the analytical second derivatives.[18c]

1. Furthermore, the analysis provides strong evidence for the preference of a closed-shell over an open-shell situation in these 14-atom anions: reorganization reactions that start out from closed-shell molecules (x = odd number) to produce two open-shell clusters (x = even number) are endoenergetic, whereas open-shell species form two closed shell anions in exoenergetic processes.

The latter is in accordance with compound **1** being EPR-silent. Thus, apart from the proposed composition, the next two closest diamagnetic compositions would be $[Ni_2Sn_9Bi_3]^{3-}$ or $[Ni_2Sn_5Bi_7]^{3-}$, both with Sn and Bi atomic numbers differing by 2 from the most likely structure. With a maximum error of ± 1 atoms to be expected for the single-crystal structure analysis, the EDX measurement, and the results of the quantum chemical investigations, this finally serves to confirm the composition of **1**.

The DFT investigations further helped to explore the bonding situation within the cluster anion in **1**, including the interaction between the two interstitial Ni atoms and those of the Ni atoms with the main-group-atom cage. However, in contrast to several intermetalloid clusters reported previously, the situation does not seem to accord to known models. Neither the Zintl–Klemm–Busmann concept[19] or a localized picture, nor Wade–Mingos[6] rules fit exactly. In the following, all three will be given a brief discussion.

The three external Sn atoms that are part of the disordered, external square faces of the $[Ni_2Sn_7Bi_5]^{3-}$ anion in **1** might be assigned the charge-carrying Sn^- anion, thus as isoelectronic *pseudo* Bi atoms; nevertheless, the topology does not accord to the Zintl–Klemm–Busmann concept regarding the number of bonds per atom, which is larger than three throughout.

The cluster may instead be viewed as an electron-precise, dinuclear intermetallic complex that is dominated by the Ni–E bonding, similar to that discussed for structurally related Ru compounds Bi_4RuBr_2 and $Bi_{24}Ru_3Br_{20}$,[20] with {BiBr} fragments isolobal to Sn, and Bi atoms equal to (Bi or) Sn^- in **1**: The $[Sn_7Bi_5]^{3-}$ binary "ligand" shell would provide 32 electrons for the bonding: 8 from the 4 Sn atoms of the central Sn_4 ring, and 24 from the 8 remaining Sn^-/Bi atoms. Assuming the tendency towards an electron count of 18 for the transition metal, each Ni atom would accept eight electrons from eight coordinating Sn/Bi atoms for eight two-center–two-electron (2c2e) Ni–E bonds. Accordingly, 16 electrons would remain for E–E bonding, used for eight 2c2e bonds in the outer squares. To verify/falsify this localized model, the chemical bonding in the cluster anion in **1** was analyzed by creating localized molecular orbitals (LMOs; see the Supporting Information) from the DFT wave function of the favorite isomer. Indeed, eight 2c2e E–E bonds can be detected in the upper and lower square faces. However, most of the Ni–E interactions do not represent 2c2e bonds according to the LMOs, but rather form delocalized multicenter bonds, also including the Sn and Bi lone pairs and the Ni–Ni bond. The existence of Ni–Ni bonding MOs contradicts the localized model that once more does not explain the short Ni–Ni contact in terms of a chemical bond, as there would be no electrons available for bond formation.

Thus, as an alternative, we have performed an analysis of the delocalized molecular orbitals (MOs; see the Supporting Information) as derived from the DFT calculation of the preferred isomer. Apart from MOs that represent multicenter Ni–E and E–E bonds, cluster orbitals and MOs can also be observed that are attributed to the Ni–Ni bond. Figure 4 shows the MO diagram for the valence orbitals of the

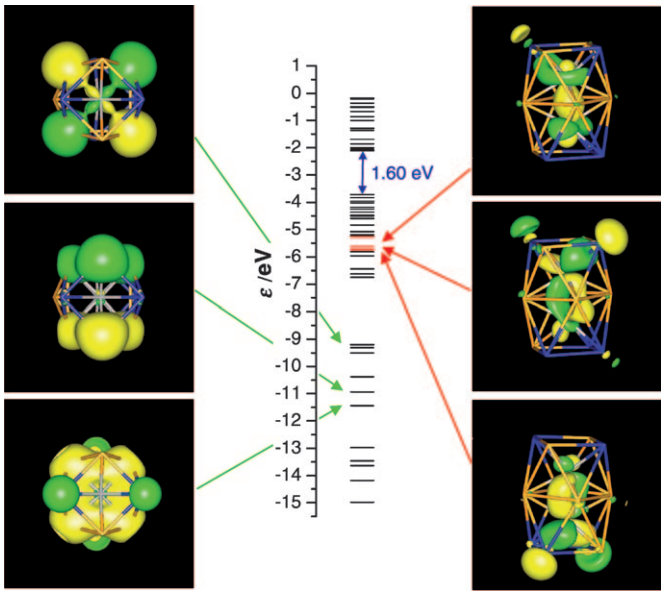

Figure 4. MO diagram of the valence orbitals of the cluster anion in **1** resulting from DFT calculations of the preferred $[Ni_2Sn_7Bi_5]^{3-}$ isomer and illustration of the electron densities (drawn to 0.2 $e^-Å^{-3}$; Ni gray, Sn orange, Bi blue)[22] as calculated for the cluster orbitals (left-hand side, viewed along the Ni–Ni bond) HOMO−26 (−9.198 eV, d character, top), HOMO−31 (−10.933 eV, p character, center), HOMO−32 (−11.434 eV, s character, bottom), and Ni–Ni bonding orbitals (right-hand side) HOMO−18 (−5.277 eV, top), HOMO−19 (−5.638 eV, center), and HOMO−20 (−5.749 eV, bottom).

preferred isomer (see Figure 3), three typical cluster MOs, and the three bonding MOs that contribute to the Ni–Ni interaction. According to a Mulliken population analysis,[21] the electronic contribution from Ni atomic orbitals to these MOs amount to 0.69 (HOMO-18, σ-type), 0.63 (HOMO-20, π-type), and 0.53 (HOMO-19, π-type), thus adding up to a total of 1.85 electrons, which is close to 2.00.

Despite the strong evidence for a delocalized bonding situation, application of Wade–Mingos rules to the cluster anion in **1**, regarding it as an *arachno* deltahedral fragment, also results in a mismatch: an *arachno* cluster with n vertices requires $2n+6$ electrons to accomplish the cluster skeleton bonding. With two extra electrons (exo) per vertex, the total electron number needed for a ligand-free 12-atom cage thus amounts to $(2\times12+6)+(2\times12)=54$ electrons. Although the interstitial Ni^0 atoms do not contribute to the cluster electrons, the atoms of the Sn_7Bi_5 cage in $[Ni_2Sn_7Bi_5]^{3-}$ provide $(7\times4)+(5\times5)=53$ electrons; the charge adds another three electrons. The resulting sum of 56 surpasses the required electron number by two electrons. This mismatch could be easily compensated for by increasing the Sn/Bi

composition by two tin atoms as $[Ni_2Sn_9Bi_3]^{3-}$, which unambiguously contradicts all other findings. Thus, the title compound represents an *arachno*-cage with $2n+8$ skeletal electrons, in violation of the Wade–Mingos rules. Very recently, the intermetalloid cluster anion $[Ir@Sn_{12}]^{3-}$, an icosahedral stannaspherene cage endohedrally filled by an Ir atom, was reported.[23a] This anion is in accordance with Wade–Mingos rules for a *closo* deltahedron. Thus, the architecture observed in **1** is an unprecedented alternative for an isolated 12-atom cage, which, however, resembles a structural fragment of the intermetallic compound Ir_3Sn_7.[23b]

In summary, both the electron number and the topology, including the uncommon square faces, disagree with the known features of Zintl anions observed to date. Therefore, we suggest regarding the anion as a cluster which accommodates the two extra electrons in a delocalized cluster orbital of low energy as the best model. A similar case of non-classifiable systems was discussed very recently for a species comprising an Al_6 moiety.[24]

Reactions of homoatomic $[E^{14}_9]^{4-}$ or $[E^{15}_7]^{3-}$ Zintl anions with Ni^0 compounds has produced a variety of different results. Treatment with $[Ni(CO)_2(PPh_3)_2]$ leads to the formation of $[Ni@(Ge_9Ni{-}PPh_3)]^{2-}$,[25] $[Ni@(Sn_9Ni{-}CO)]^{2-}$,[26] or $[\{Ni(CO)_2\}_2(\mu\text{-}Si_9)_2]^{8-}$[27] with $[E_9]^{4-}$ anions as ligands to Ni complex fragments. Syntheses using $[Ni(cod)_2]$ yield intermetalloid cluster anions that comprise one to three Ni atoms, $[Ni@Pb_{10}]^{2-}$,[3] $[Ni@Pb_{12}]^{2-}$,[3] $[Ni_2@Sn_{17}]^{4-}$,[28] and $[Ni_3@(Ge_9)_2]^{4-}$.[16] Finally, the unique, onion-type icosahedral cluster $[As@Ni_{12}@As_{20}]^{3-}$ cited above was obtained by a reaction of $[As_7]^{3-}$ with $[Ni(cod)_2]$.[5] A Ni–Ni dumbbell was not observed in any of these examples. Similar arrangements have only been reported for Pd and Pt in $[Pd_2@E_{18}]^{4-}$ (E = Ge[4], Sn[29,30]) and $[Pt_2@Sn_{17}]^{4-}$.[31] However, in contrast to **1**, these species are closed deltahedra and do not feature square faces. Thus, by using binary E^{14}/E^{15} precursor, the resulting molecular structure is an unprecedented variation of the structural features.

Apart from the described structural peculiarities observed in compound **1**, our observations lead to the conclusion that in mixed E^{14}/E^{15} and $M/E^{14}/E^{15}$ anions, the main-group element that is in the majority has the dominant structure-directing influence. Accordingly, the ternary anion in **1**, containing more Group 14 than Group 15 element atoms, shows basic structural features that have been observed with binary M/E^{14} anions, whereas the reported ternary anions $[Zn_6Sn_3Bi_8]^{4-}$ and $[Sn_2Sb_5(ZnPh)_2]^{3-}$ are more closely related to structures that were previously observed with Group 15 elements. However, the "electronic flexibility" that is introduced by the other element type leads to structural deviations and novelties, the exploration of which is currently the subject of comprehensive experimental and theoretical work.

Experimental Section

All manipulations and reactions were performed under an Ar or dry N_2 atmosphere using standard Schlenk or glovebox techniques. $[K([2.2.2]crypt)]_2[Sn_2Bi_2]\cdot en$ was prepared according to the literature.[12] All solvents were dried, freshly distilled and stored under Ar prior to use. [2.2.2]crypt[32] (Merck) and $[Ni(cod)_2]$ (Acros Organics) were dried in vacuum for 13 h.

1: $[K([2.2.2]crypt)]_2[Sn_2Bi_2]\cdot en$ (193 mg, 0.125 mmol) was weighed out into a Schlenk tube inside a glovebox and dissolved in en (3 mL). The color of this solution is dark reddish brown. In another Schlenk tube inside a glovebox, $[Ni(cod)_2]$ (44 mg, 0.163 mmol) was weighed out and suspended in en (1 mL) to give a colorless suspension. This suspension was added to the dark-reddish brown solution while stirring powerfully. The reaction mixture was allowed to stir for 3 h. The dark brown reaction solution was filtered through a standard glass frit and carefully layered by toluene (5 mL). After 2 days, dark brown plates of **1** crystallized on the wall of the Schlenk tube in approximately 15% yield based on the starting material. Semi-quantitative energy-dispersive X-ray spectroscopy (EDX) analyses of several crystals confirmed the composition of **1** (see below). The starting material $[K([2.2.2]crypt)]_2[Sn_2Bi_2]\cdot en$ was observed as a second crystalline product.

Single-crystal X-ray data collection was performed using a Stoe IPDS2T diffractometer at 100 K with $Mo_{K\alpha}$ radiation and graphite monochromatization. Structure solution was realized by direct methods, refinement with full-matrix-least-squares against F^2 using SHELXS-97 and SHELXL-97 software.[33,34] For details, see the Supporting Information. CCDC 768360 (**1**) contains the supplementary crystallographic data for this paper. These data can be obtained free of charge from The Cambridge Crystallographic Data Centre via www.ccdc.cam.ac.uk/data_request/cif.

For the ESI-MS studies, a Finnigan LTQ-FT spectrometer (Thermo Fischer Scientific) was used in the negative-ion mode (spray voltage 3.90 kV, capillary temperature 300 °C, capillary voltage −11 V, tube lens voltage −108.38 V, with sheath gas flow.

DFT[17] investigations of the anionic molecules were undertaken using the program system TURBOMOLE[18] (RIDFT program,[35] Becke–Perdew 86 (BP86) functional,[36] grid size m3). Basis sets were of def2-TZVP quality (TZVP = triple-zeta valence plus polarization).[37] For Sn (ECP-28)[38] and Bi atoms (ECP-60),[38] effective core potentials were used for consideration of relativistic corrections and to reduce the computational effort. The high negative charge was compensated for by employment of the COSMO model.[39] Further details are provided in the Supporting Information.

Received: September 2, 2010
Published online: December 10, 2010

Keywords: density functional calculations · intermetalloid clusters · mass spectrometry · structure elucidation · Zintl anions

[1] a) H. Schnöckel, *Dalton Trans.* **2008**, *33*, 4344–4362; b) T. F. Fässler, S. D. Hoffmann, *Angew. Chem.* **2004**, *116*, 6400–6406; *Angew. Chem. Int. Ed.* **2004**, *43*, 6242–6247.
[2] N. Korber, *Angew. Chem.* **2009**, *121*, 3262–3264; *Angew. Chem. Int. Ed.* **2009**, *48*, 3216–3217.
[3] E. N. Esenturk, J. Fettinger, B. Eichhorn, *J. Am. Chem. Soc.* **2006**, *128*, 9178–9186.
[4] J. M. Goicoechea, S. C. Sevov, *J. Am. Chem. Soc.* **2005**, *127*, 7676–7677.
[5] M. J. Moses, J. C. Fettinger, B. W. Eichhorn, *Science* **2003**, *300*, 778–780.
[6] a) K. Wade, *Adv. Inorg. Chem. Radiochem.* **1976**, *18*, 1–67; b) D. M. P. Mingos, *Nat. Phys. Sci.* **1972**, *236*, 99–102; c) D. M. P. Mingos, *Acc. Chem. Res.* **1984**, *17*, 311–319.
[7] J. M. Goicoechea, S. C. Sevov, *Angew. Chem.* **2006**, *118*, 5271–5274; *Angew. Chem. Int. Ed.* **2006**, *45*, 5147–5150.
[8] B. Zhou, M. S. Denning, D. L. Kays, J. M. Goicoechea, *J. Am. Chem. Soc.* **2009**, *131*, 2802–2803.

[9] J.-Q. Wang, S. Stegmaier, T. F. Fässler, *Angew. Chem.* **2009**, *121*, 2032 – 2036; *Angew. Chem. Int. Ed.* **2009**, *48*, 1998 – 2002.

[10] F. Lips, S. Dehnen, *Angew. Chem.* **2009**, *121*, 6557 – 6560; *Angew. Chem. Int. Ed.* **2009**, *48*, 6435 – 6438.

[11] F. Lips, I. Schellenberg, R. Pöttgen, S. Dehnen, *Chem. Eur. J.* **2009**, *15*, 12968 – 12973.

[12] S. C. Critchlow, J. D. Corbett, *Inorg. Chem.* **1982**, *21*, 3286 – 3290.

[13] ESI-MS investigations that were performed at earlier states of the reaction indicate different relative amounts of the detectable fragments and further fragments to appear. We ascribe these findings to complicated equilibria that appear during the reaction. Therefore, comprehensive analyses on the formation process are currently being undertaken using ESI mass spectrometry in combination with theoretical studies; these will be subject of another publication dedicated exclusively to this point.

[14] It was not possible to assign all of the observed peaks to reasonable species, as some of them contain fragments of solvent and/or cryptand molecules along with cluster atoms; however, the isotopic pattern enables the assignment of the number of Sn atoms, indicating two Sn atoms for the highest paek at *m*/*z* 916.9034, for example.

[15] a) J. D. Corbett, P. A. Edwards, *J. Am. Chem. Soc.* **1977**, *99*, 3313 – 3317; b) S. C. Critchlow, J. D. Corbett, *J. Am. Chem. Soc.* **1983**, *105*, 5715 – 5716; c) T. F. Fässler, *Coord. Chem. Rev.* **2001**, *215*, 347 – 377; d) S. C. Sevov, J. M. Goicoechea, *Organometallics* **2006**, *25*, 5678 – 5692, and references therein.

[16] J. M. Goicoechea, S. C. Sevov, *Angew. Chem.* **2005**, *117*, 4094 – 4096; *Angew. Chem. Int. Ed.* **2005**, *44*, 4026 – 4028.

[17] a) R. G. Parr, W. Yang, *Density Functional Theory of Atoms and Molecules*, Oxford University Press, New York **1988**; b) T. Ziegler, *Chem. Rev.* **1991**, *91*, 651 – 667.

[18] a) R. Ahlrichs, M. Bär, M. Häser, H. Horn, C. Kölmel, *Chem. Phys. Lett.* **1989**, *162*, 165 – 169; b) O. Treutler, R. Ahlrichs, *J. Chem. Phys.* **1995**, *102*, 346 – 354; c) The program AOFORCE inplemented in TURBOMOLE was used for the calculation of second derivatives.

[19] a) E. Zintl, *Angew. Chem.* **1939**, *52*, 1 – 6; b) W. Klemm, *Proc. Chem. Soc. London* **1959**, 329 – 341; c) E. Busmann, *Z. Allg. Anorg. Chem.* **1961**, *313*, 90 – 106; d) *Chemistry*, *Structure and Bonding of Zintl Phasses and Ions*, (Ed.: S. M. Kauzarich), VCH, New York, **1996**.

[20] a) M. Ruck, *Z. Anorg. Allg. Chem.* **1997**, *623*, 1583 – 1590; b) M. Ruck, *Z. Anorg. Allg. Chem.* **1997**, *623*, 1591 – 1598.

[21] R. S. Mulliken, *J. Chem. Phys.* **1955**, *23*, 1833 – 1840.

[22] gOpenMol, Leif Laaksonen, Center for Scientific Computing, Espoo, Finland, Version 3.0, **2005**.

[23] a) J.-Q. Wang, S. Stegmaier, B. Wahl , T. F. Fässler, *Chem. Eur. J.* **2010**, *16*, 1793 – 1798; b) H. Nowotny, K. Schubert, U. Dettinger, *Metallforschung* **1946**, *1*, 137 – 145.

[24] P. Henke, N. Trapp, C. E. Anson, H. Schnöckel, *Angew. Chem.* **2010**, *122*, 3214 – 3218; *Angew. Chem. Int. Ed.* **2010**, *49*, 3146 – 3150.

[25] D. R. Gardner, J. C. Fettinger, B. W. Eichhorn, *Angew. Chem.* **1996**, *108*, 3032 – 3033; *Angew. Chem. Int. Ed. Engl.* **1996**, *35*, 2852 – 2854.

[26] B. Kesanli, J. Fettinger, D. R. Gardner, B. Eichhorn, *J. Am. Chem. Soc.* **2002**, *124*, 4779 – 4786.

[27] S. Joseph, M. Hamberger, F. Mutzbauer, O. Härtl, M. Maier, N. Korber, *Angew. Chem.* **2009**, *121*, 8926 – 8929; *Angew. Chem. Int. Ed.* **2009**, *48*, 8770 – 8772.

[28] E. N. Esenturk, J. C. Fettinger, B. W. Eichhorn, *J. Am. Chem. Soc.* **2006**, *128*, 12 – 13.

[29] Z.-M. Sun, H. Xiao, J. Li, L.-S Wang, *J. Am. Chem. Soc.* **2007**, *129*, 9560 – 9561.

[30] F. S. Kocak, P. Zevalij, Y.-F. Lam, B. W. Eichhorn, *Inorg. Chem.* **2008**, *47*, 3515 – 3520.

[31] B. Kesanli, J. E. Halsig, P. Zevalij, J. C. Fettinger, B. W. Eichhorn, *J. Am. Chem. Soc.* **2007**, *129*, 4567 – 4574.

[32] [2.2.2]crypt: 4,7,13,16,21,24-Hexaoxa-1,10-diazabicyclo-[8.8.8]hexacosane.

[33] G. W. Sheldrick, SHELXTL 5.1, Bruker AXS Inc., **1997**.

[34] X-ray data for $C_{71.63}H_{138.52}Bi_{4.5}K_3N_{9.63}Ni_2O_{18}Sn_{7.5}$ (**1**): monoclinic, space group *Cc*, $a = 29.747(6)$, $b = 13.075(3)$, $c = 28.220(6)$ Å, $\beta = 107.13(3)°$, $V = 10489(4)$ Å^3, $Z = 4$, R_1 $(I > 2\sigma(I)) = 0.0540$, wR_2 (all data) = 0.1457, GooF (all data) 1.042, max. peak/hole 2.497/−2.928.

[35] a) K. Eichkorn, O. Treutler, H. Öhm, M. Häser, R. Ahlrichs, *Chem. Phys. Lett.* **1995**, *242*, 652 – 660; b) K. Eichkorn, F. Weigend, O. Treutler, R. Ahlrichs, *Theor. Chim. Acta* **1997**, *97*, 119 – 124.

[36] a) A. D. Becke, *Phys. Rev. A* **1988**, *38*, 3098 – 3109; b) S. H. Vosko, L. Wilk, M. Nusair, *Can. J. Phys.* **1980**, *58*, 1200 – 1205; c) J. P. Perdew, *Phys. Rev. B* **1986**, *33*, 8822 – 8837.

[37] F. Weigend, R. Ahlrichs, *Phys. Chem. Chem. Phys.* **2005**, *7*, 3297 – 3305.

[38] B. Metz, H. Stoll, M. Dolg, *J. Chem. Phys.* **2000**, *113*, 2563 – 2569.

[39] a) A. Klamt, G. Schürmann, *J. Chem. Soc. Perkin Trans.* **1993**, *5*, 799 – 805; b) A. Schäfer, A. Klamt, D. Sattel, J. C. W. Lohrenz, F. Eckert, *Phys. Chem. Chem. Phys.* **2000**, *2*, 2187 – 2193.

